Proceedings of the 25th International Conference on
Port and Ocean Engineering under Arctic Conditions
June 9-13, 2019, Delft, The Netherlands

Hydrostatic Weighing Method in Application to Model Ice Density Measurements

Tatiana Zvyagina[1], Petr Zvyagin[1,2]
[1] Peter the Great St. Petersburg Polytechnic University, St. Petersburg, Russia
[2] Krylov State Research Centre, St. Petersburg, Russia

ABSTRACT

Model ice, which is used nowadays in ice tanks, has a soft bottom layer. This obstructs defining ice specimen volume without special equipment. The application of usual mass/volume method may lead to a significant error and scatter of results.

The paper analyzes the method of hydrostatic weighing for model ice density measurement (method C from the corresponding ITTC recommendations). This method allows calculating density with the use of weighing scales and water basin only. Hand submerging of the specimen was applied, so no additional installations were demanded.

To study the observational error, preliminary experiments with monophase paraffin specimen were performed. The formula of density used in hydrostatic method was expanded to Maclaurin series. Influence of observational error in the third weighting of method C tends to decrease with increasing of the specimen mass. With careful performance this type of error can contribute less than 3 kg/m^3 to resulting density value when using specimen of about 1 kg mass.

The speed of brine drainage from model ice specimens was investigated. Fine Grain model ice fields in Krylov State Research Centre ice tank were used. The amount of drained water in the first minute is found to be governed by logarithmic law. With increasing mass of the specimen the velocity of drainage increased. After submersion of the specimen the velocity of drainage increased as well. The brine drainage can subtract 4 kg/m^3 from density value in the first 30 seconds when measuring 0.035 m thick model ice specimen of about 1 kg mass.

KEY WORDS: Model ice, density, measurement error, ice tank.

NOMENCLATURE

w_1 – mass of basin with water, kg;

w_2 – mass of basin with water and floating ice specimen, kg;

w_3 – mass of basin with water and submerged ice specimen, kg;

w_s – mass of ice sample, kg;

ρ – model ice density;

ρ_t – true bulk density of specimen material;

ρ_w – water density, kg/m^3;

Δ_i – scatter of measurements of the value of w_3, in two independent experiments;

w_3^* – true value of w_3 for paraffin specimen;

x – value of w_3 indication reading error while submerging specimen by hand.

INTRODUCTION

Sea ice is anisotropic multiphase material; its properties depend on temperature, density, salinity and porosity (Loset et al., 2010). Sea ice contains several components: solid ice, brine, air and admixtures. Each component influences the resulting density of the material. Timco and Frederking (Timco and Frederking, 1996) indicate the range 720 – 940 kg/m^3 for sea ice density and note that densities of ice below and above waterline are different. For the first year ice the ranges for density are 840 – 910 kg/m^3 above the waterline and 900 – 940 kg/m^3 below the waterline. The reason for wide ranges is that measurements were made in different regions with different weather conditions and water salinity. Another reason for scatter is variety of methods for density measurement: if a specimen is extracted from the floating field, then brine drainage from it occurs and the overall density of the specimen is changed.

Cox and Weeks (1983) developed expressions for estimating sea ice density at different temperature and salinity. They generalized data on density/temperature/salinity (Table 1) which indicates that the ice density increases as the salinity increases.

Table 1. Calculated rounded densities of gas-free sea ice at different salinities, kg/m^3, at temperatures −2°C and −8°C according to the paper by Cox and Weeks (1983)

Salinity, ‰	1	2	5	10	20
T=−2°C					
Zubov (1945)	922	926	930	939	
Anderson (1960)	919.8	925.2	930.7	944.7	973.9
Schwerdtfeger (1963)	919.1	923.3	927.5	937.9	958.8
Cox&Weeks (1983)	920	925.4	930.8	944.8	974
T=−8°C					
Zubov (1945)	920	923	925	932	944
Anderson (1960)	919.2	921.6	924	930.1	942.6
Schwerdtfeger (1963)	917.5	918.6	919.6	922.2	927.5
Cox&Weeks (1983)	919.3	921.8	924.2	930.3	942.9

The data on porosity and permeability of sea ice is scarce (Cox and Weeks, 1983), (Petrich and Sun, 2006), though these parameters are connected with density of ice in floating and submerged positions.

Li and Riska analyzed model ice used at Aalto University ice tank (Li and Riska, 2002) and noted that in comparison with the fresh water ice and sea ice the density of the model ice is higher. Later von Bock und Polach et al. (2013) reported the density of model ice in Aalto University ice tank to be 911 kg/m^3.

Model ice density is important for model-scale ice experiments processing, because density of unbroken floes and broken submerged model ice governs buoyancy forces. Also knowledge of density is important for estimating the mass of ice features in model and natural conditions.

METHOD OF DENSITY MEASUREMENTS AND EXPERIMENTAL MATERIALS

Several methods are used for ice density measurements. Well known mass/volume method is applicable for measuring ice density ρ in field conditions (Timco and Weeks, 2010) as well as in ice tanks (ITTC, 2014). Mass/volume is a simple method, but it has some weaknesses. It is usually almost impossible to take in account all amount of water and brine, which leaking out of a specimen, if its mass is measured after extracting from the natural environment. For volume measurement it is usually requires a specimen of a regular geometrical shape, which is difficult in the case of soft model ice.

In this paper a hydrostatic weighing method for ice density measurements is considered. This method is recommended by ITTC for using in ice tanks (ITTC, 2014); it is also applicable to measure ice density in field conditions (Pustogvar, 2016). The method of hydrostatic weighing consists of the following steps (Fig. 1):

1) basin with water from the tank is prepared and weighed;
2) ice specimen is put into the basin, after that the basin with the floating specimen is weighed for the second time;
3) the specimen is submerged into the water as it is shown in Fig. 1 and the third weighing is performed.

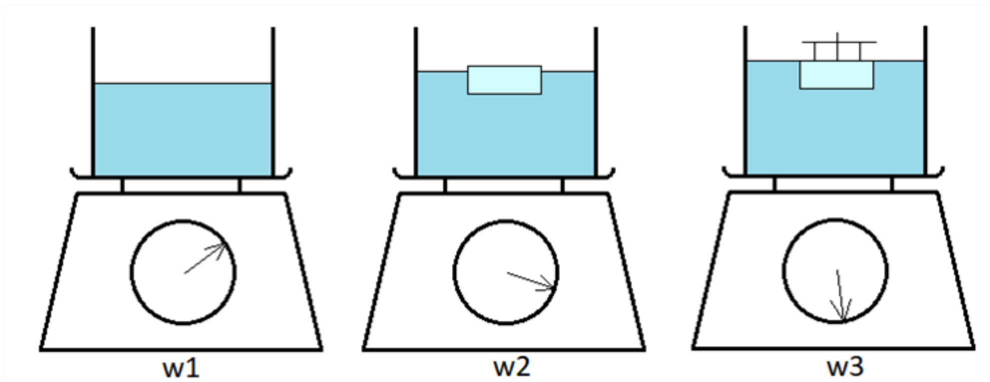

Figure 1. Hydrostatic method of model ice density measurement (ITTC, 2014)

Model ice specimen density ρ is found from the formula:

$$\rho = \frac{w_2 - w_1}{w_3 - w_1} \cdot \rho_w \quad (1)$$

The advantage of this method is that only mass need to be weighted, with no need for providing a regular shape for the ice specimen.

There are no conventional recommendations on specimen submersion as far as the authors are aware. We used submersion by hand as it is shown in Fig. 2 (here it is applied to paraffin specimen, which will be considered later). Submersion by hand in a rubber glove is a simple operation and does not require special equipment. However, this approach leads to an error in reading the value of w_3. This error will be studied below.

Figure 2. Paraffin specimen submersion performed by hand

Model ice specimens were tested in Krylov State Research Centre (St. Petersburg). In the new ice tank the model ice is prepared according to Fine Grain technology (Timofeev et al., 2015). Some mechanical parameters of model ice floes prepared in the ice tank of Krylov State Research Centre can be found in the earlier paper (Zvyagin, 2016).

ERROR IN WEIGHT MEASUREMENTS IN SUBMERGED POSITION

The samples of FG-model ice, used in Krylov State Research Centre, have deformable structure, uneven slushy bottom surface and cells from which water or brine can leak out when the sample is extracted from the ice field. For instance, model ice used in the ice tank of Aalto University (Espoo, Finland) has similar properties (Von Bock und Polach and Kujala, 2013).

To estimate the parameters of scales indication error while measuring weight w_3, a number of experiments with paraffin sample were performed. Unlike the FG model ice, the sample made of paraffin is solid, relatively firm and does not have cells with brine. Values of w_1 и ρ_w remain constant in both types of the experiment – with model ice and paraffin. Readings of value w_2 in the experiments with model ice had an error because of brine leaking out. In the experiments with paraffin sample the value w_2 remained constant.

Paraffin brick sample of 0.575 kg mass was used. To estimate variation of w_3 60 measurements with paraffin sample were performed in same conditions by both of the the authors independently. Let us define with $w_{1.i}$ and $w_{2.i}$ values of w_1 and w_2 measured in i-th experiment; with $w_{3.1i}$ and $w_{3.2i}$ – measurements of w_3, made in i-th experiment by the first and the second author, respectively. Measurements were made in the following order: $w_{1.i}$, $w_{2.i}$, then independently $w_{3.1i}$ and $w_{3.2i}$, then amount of water in basin was changed and all the procedure was repeated.

Let us consider the following discrepancies:

$$\Delta_i = (w_{3.1i} - w_{3.2i}) \quad (2)$$

They characterize scatter occurred when value w_3 is measured in unstable position of a paraffin brick, which is held under the water surface by the hand in a rubber glove. In 60 experiments the sample of Δ_i of size 60 was obtained. Sample average was -0.0007 kg, sample standard deviation was 0.0024 kg, sample histogram is presented in Fig. 3. Average of absolute values $|\Delta_i|$ was 0.0019 kg. Based on Fig. 3 we can put forward hypothesis that Δ_i has Gaussian distribution. According to this we can say it is unlikely that absolute value of Δ_i will exceed 0.008 kg if such experiment will be performed in same conditions.

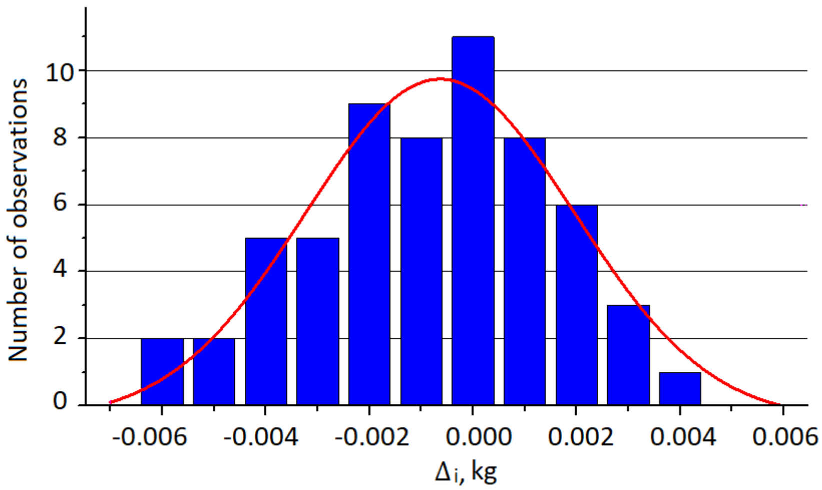

Figure 3. Histogram of sample of Δ_i in the experiments with paraffin specimen

Let us denote with w_3^* – the true value of w_3 for this particular paraffin specimen in given conditions, and with x – the value of w_3 indication reading error while submerging specimen by hand. This way:

$$w_3 = w_3^* + x \tag{3}$$

Let us think that x is small. For the paraffin specimen we can get rather reliable estimator of w_3^*. For that we use 120 observations $w_{3.1i}$, $w_{3.2i}$, $i = 1..60$ obtained before, get sample of 120 paraffin density values, find sample average density $\tilde{\rho} = 884{,}65$. This way we can estimate value of w_3^* for each i-th measurement using (1):

$$w_{3.i}^* \approx w_{1.i} + \frac{\rho_w}{\tilde{\rho}} 0.575 \tag{4}$$

From (3) and (4) the sample of x of size 120 was obtained, histogram of it is presented in Fig. 4. Average x was –0.00001 kg, sample standard deviation was 0.002 kg. We can put forward hypothesis that x has Gaussian distribution. Then we can suggest it is unlikely that absolute value of x will exceed 0.006 kg.

Let us explore how error x influences density ρ calculated by (2). We can expand (2) with respect of (4) by Maclaurin formula:

$$\rho(x) = \frac{w_2 - w_1}{w_3^* + x - w_1} \cdot \rho_w = \left(\frac{w_2 - w_1}{w_3^* - w_1}\right) \cdot \rho_w \cdot \left(1 - \frac{x}{w_3^* - w_1}\right) + R_2(x) \tag{5}$$

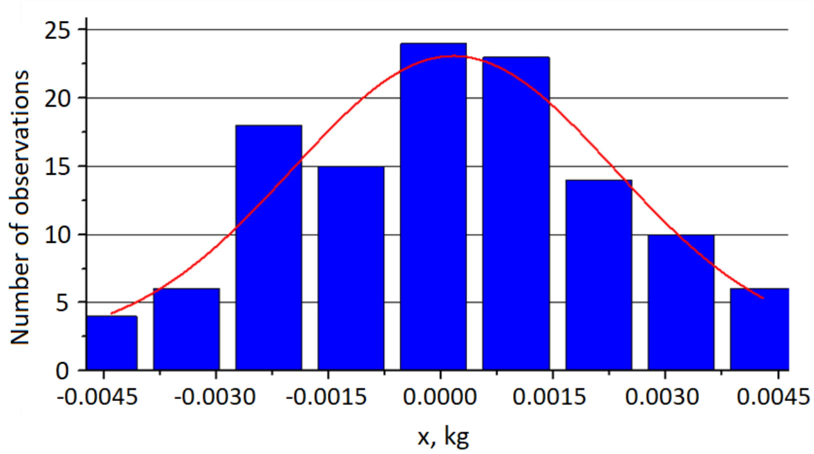

Figure 4. Histogram of w_3 measurement error x obtained in the experiment with paraffin specimen

Here $R_2(x)$ is remainder in the Lagrange's form. If value of x is small, then we can expect that $R_2(x)$ will be small as well.

$$R_2(x) = \frac{(w_2 - w_1)\cdot\rho_w}{(w_3^* - w_1 + \theta)^3}\cdot x^2, \quad 0 < \theta < x \tag{6}$$

Let us denote a weight of specimen as w_s

$$w_s = w_2 - w_1 \tag{7}$$

If we denote with ρ_t the true bulk density of specimen material we can rewrite (6) in the following way:

$$\rho(x) = \rho_t - \frac{x}{\rho_w w_s}\rho_t^2 + R_2(x) \tag{8}$$

In the case of small $R_2(x)$ the discrepancy of calculated density value with true unknown density value is:

$$|\Delta\rho(x)| \approx \frac{|x|}{\rho_w w_s}\rho_t^2 \tag{9}$$

Considering the experiment with paraffin we have taken an estimator $\tilde{\rho} = 884.65$ kg/m^3 as ρ_t, while $w_s = 0.575$, this way we found out that absolute value of $R_2(x)$ has not exceeded 0.055 kg/m^3. At the same time the $|\Delta\rho(x)|$ value (10) has not exceed 7 kg/m^3.

One can compare values of $|\Delta\rho(x)|$ and $|R_2(x)|$, which are provided for the range of x and for different weights w_s of specimen while $\rho_t = 900$ kg/m^3 and $\rho_w = 1009$ kg/m^3 in the Fig. 5.

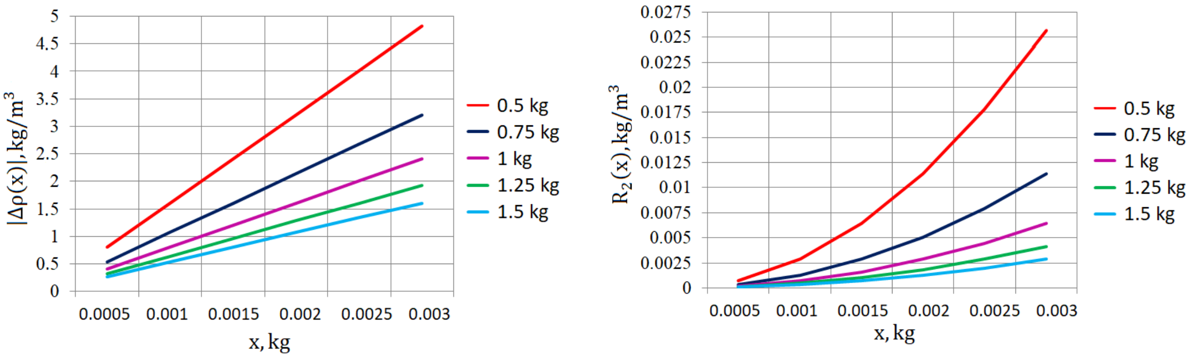

Figure 5. Plots of $|\Delta\rho(x)|$ (10) and $|R_2(x)|$ for $\rho_t = 900\ \mathrm{kg/m^3}$, $\rho_w = 1009\ \mathrm{kg/m^3}$ and different weights of a specimen

We can say that value of $R_2(x)$ can be percept as insignificant in comparison with $\Delta\rho(x)$. Also we can conclude, that $|\Delta\rho(x)|$ and $|R_2(x)|$ both decrease with increasing of the specimen weight. This way, large ice specimens are more preferable for testing than small ones.

VELOCITY OF BRINE DRAINAGE

Model Fine Grain ice is a porous material as well as a real ice. Pores of sea ice are filled with brine and air (Cox and Weeks,1983), as well as pores of model ice.

When the model ice specimen is extracted from its natural position in a floating ice floe, the brine begins to leak out from pores and an air begins to occupy brine's place. Because of that we can expect that model ice density in natural conditions and after extraction will be different. On the other hand the hydrostatic method is not possible without extracting the specimen of ice from the water basin.

We understand brine drainage velocity as a first derivative of a mass, which depends on time. The following experiments were performed to estimate the rate of brine drainage and to find out how density of extracted specimen changes with time. The floating model ice specimen, separated from the level model ice floe, was scooped up with surrounding water by the small basin. The basin was put on the scales and measuring of the weight w_2 was performed. Then the specimen was taken out of the water with hand in a rubber glove and held in horizontal position for 50 seconds as it is shown in Fig. 6.

Figure 6. Measuring the rate of water draining from the ice specimen

Water/brine leaked out to the basin and during that time the video recording of basin weight indication was made. After 50 seconds the specimen was carefully put back to the basin, and then the whole procedure was repeated with the same specimen and the same amount of water. Air temperature during experiments was -5 − -6°C, The temperature of surface layer was about melting point, which is -0.6°C (Popov et al., 1979) for water of measured salinity. The results of five different specimen testing experiments are provided in Table 2. In the following figures these model ice specimens will be denoted with the same numbers.

Table 2. Test results on water/brine drainage of ice specimen (unsubmerged)

Number of specimen	1	2	3	4	5
Ice thickness, m	0.029	0.03	0.029	0.034	0.035
Weight $\boldsymbol{w_2}$, kg	4.599	4.53	3.922	4.843	4.918
Weight $\boldsymbol{w_3}$ (estimate), kg	4.662	4.619	4.019	4.954	5.028
Estimate of sample mass in natural environment, kg	0.718	0.881	0.991	1.072	1.118
Estimate of water leaked out after 50 sec, kg	0.0187	0.0195	0.0207	0.027	0.03

We were expecting that porous structure of a specimen upper surface can detain water, so the second part of the experiment was performed for determining the ability of ice sample to detain water after its submersion. The specimen was submerged with a hand in a rubber glove, and weight w_3 was measured in this position. Then the sample was taken out and held for 50 seconds with water draining to the basin, while basin weight was recorded. Several experiments with draining after specimen submersion were performed with each specimen except for the second one because of its sudden failure.

This way a number of curves for basin weight dynamics were obtained. To estimate the brine drainage velocity it is useful to adjust a function to experimental curves. We have chosen the following logarithmic function for this purpose:

$$x(t) = b + a\ln t, \text{ while } t > 0 \tag{10}$$

where t – time and x – weight on the scales.

Parameters a and b were estimated according to Least square method (LSQ):

$$b = \frac{\sum_{i=1}^{N} x_i - a\sum_{i=1}^{N} \ln t_i}{N}, \quad a = \frac{\sum_{i=1}^{N} x_i \ln x_i - \bar{x}\sum_{i=1}^{N} \ln t_i}{\sum_{i=1}^{N} (\ln t_i)^2 - \frac{(\sum_{i=1}^{N} \ln t_i)^2}{N}} \tag{11}$$

where t_i is i-th time moment (second) of the observation, x_i – weight on scales at i-th second, N – number of time moments. Here $N = 50$. The relative discrepancy of function (10) with data was described by the formula:

$$\Delta_i = \frac{|x(t_i) - x_i|}{x_i} \times 100\% \tag{12}$$

Curves, which present Δ for ice specimen of different mass and thickness are presented in Fig. 7. The average relative discrepancy of logarithmic trend with data is less than 0,05%, so the fit can be considered as good.

In formula (10) parameter b is the approximate weight of the basin without ice sample at first second of observation, $b \approx x_1$. We can use this value as w_1 in formula (2) for model ice density estimation.

Velocity of water leaking from the model ice sample can be estimated as first derivative from the function (10); this way leaking velocity is inversely proportional to the elapsed time. Here parameter a in (10) is proportionality factor. Estimated curves of water leaking velocity for specimen of different mass and thickness are presented in Fig. 9b.

Pairs of estimated parameters (a, b) for all of experiments are presented in Fig. 8. Numbers in Fig. 8 correspond to experiment numbers in Table 2. Circular marks correspond to the experiments before sample submersion and square marks – after submersion. From Fig. 8 we can see that proportionality factors a, which are obtained in similar experiments, demonstrate scatter.

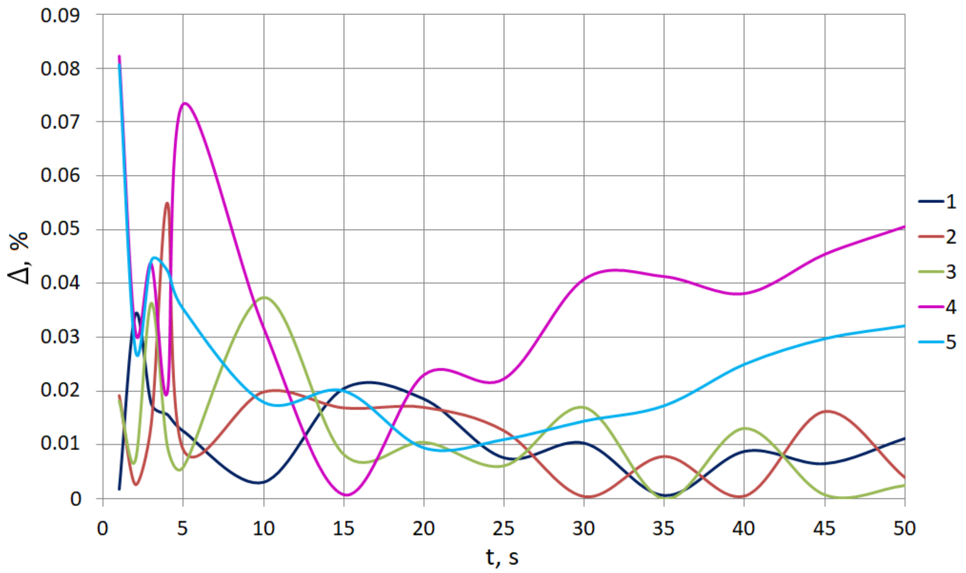

Figure 7. Relative discrepancies of average weight w_1 of empty basin with logarithmic function (water is leaking out of the sample to the basin). Curve number corresponds to experiment number in Table 2

Another important conclusion can be made from the Fig. 8: water leaking velocity after a specimen submersion is greater than without submersion. A noticeable amount of water apparently leaks into pores of the central part and upper surface of the specimen during submersion, and then leaks out when the specimen is taken out.

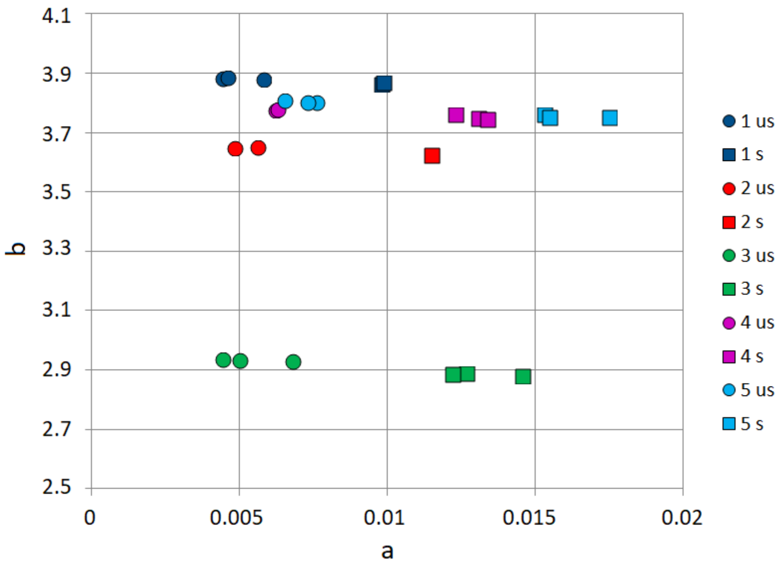

Figure 8. Parameters of adjusted logarithmic functions to dynamics of water mass in basin in experiments with water/brine drainage

Curves of average cumulative mass of water drained out of the model ice specimens in unsubmerged case are presented in Fig. 9a. It is seen that curves are grouped according to the ice thickness.

Curves, which estimate drainage velocities are presented in Fig. 9b. Functions which define these curves are found as first derivatives from (10). With solid curves the drainage velocities for unsubmerged specimen are presented, with dashed curves − drainage velocities for submerged specimen are shown. As it was expected, with iincreased mass of specimen the velocity of drainage was also increased.

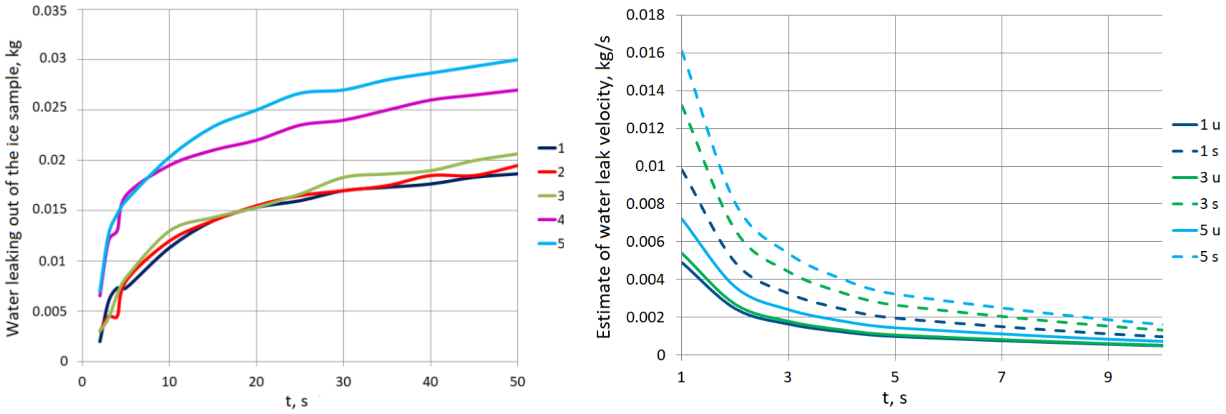

Figure 9. a) Average cumulative mass of water drained out from model ice specimens. Curve number corresponds to experiment number in Table 2; b) estimates of drainage velocities. Curve number corresponds to experiment number in Table 2

MEASURED MODEL ICE DENSITY

In Table 3 results of Fine Grain model ice density measurements in the ice tank of Krylov State Research Centre (St. Petersburg) are summarized. The specimens were taken from 4 floes. On the floe A experiments 1-3 from Table 2 were conducted, on the floe B − experiments 4-5 from Table 2 were conducted. Floes A and B are of the same field, but floe A was right at the dock part of the tank, and floe B was closer to the central part of the tank. Columns A(u), B(u) correspond to weightings, which were conducted without specimens submersion, while A(s), B(s) − to weightings after submersion. The measurements provided in column C and D were conducted in the central parts of two separate ice fields. In the experiments with the field C the water leaked freely out of the specimen for about 20 seconds while it was carried to the measuring site. Water density in these experiments was defined by the mass/volume method.

Table 3. Results of FG-ice density measurements

Test floe	A(u)	A(s)	B(u)	B(s)	C	D
Water density, kg/m^3	1015.2	1015.2	1015.2	1015.2	1009	1010.6
Number of measurements	8	6	5	6	19	7
Average measured model ice density, kg/m^3	926.7	929.7	922.1	925.2	905.9	910
Sample standard deviation of model ice density, kg/m^3	5.96	5.38	3.04	4.1	9.24	7.86
Sample range of model ice density, kg/m^3	922-933.4	924.9-935.5	920-924.3	922.3-928.1	884.3-918.7	901-915.3
Ice thickness, m	0.029-0.03	0.029-0.03	0.034-0.035	0.034-0.035	0.038	0.041-0.044
Brine drainage	No	No	No	No	Yes	No

It is seen that in average the density of model ice increased with increased water density. The submersion of the specimen described above increased its density for about 3 kg/m^3 on average.

In one of the experiments with specimen No 5 from Table 2 made from submerged position the long exposition (more than 6 min) of the sample above the basin was conducted. The curve of this specimen density, calculated with using of time moments from the range 1-370 s, is shown in Fig. 10.

It is seen that brine drainage contributes to density change of the material. The experiment was performed for specimen with mass 1.118 kg, thickness 0.035 m and water density 1015.2 $\frac{\text{kg}}{\text{m}^3}$. The density change in the period of 370 seconds was 6.1 $\frac{\text{kg}}{\text{m}^3}$. From second 1 to second 20 the loss of density was 3.69 $\frac{\text{kg}}{\text{m}^3}$. Rate of brine loss is especially important for the first minuite when the specimen is extracted from the natural environment: operations related to weighing are usually not time consuming.

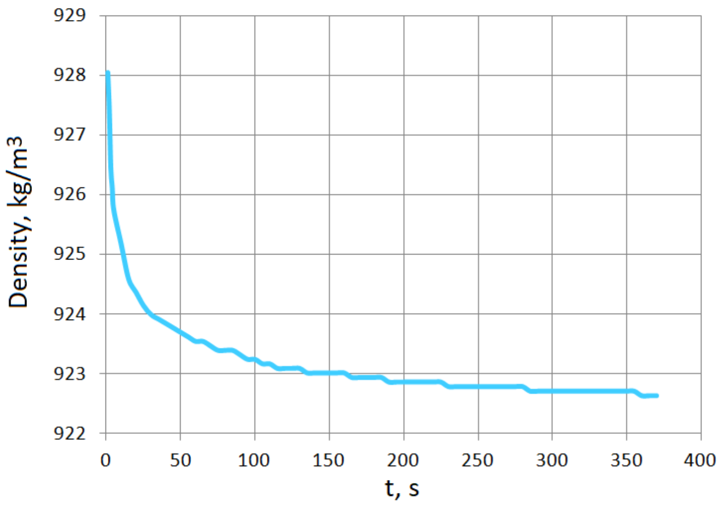

Figure 10. Estimate of the dynamics of the model ice specimen density subjected to continual drainage

CONCLUSIONS

A simple version of hydrostatic weighting method for model ice density measuring provides acceptable results. Simplification of the method consists of the following: special equipment for specimen submersion is substituted by a hand in a rubber glove. An error, which appears with that simplification, is connected with reading of weight w_3. The study of this error performed for solid paraffin specimen revealed that it is likely distributed Gaussian with zero mean.

In the paper a contribution of this possible error to resulting calculated density value is studied. It is revealed that with specimen of weight 1 kg and more the contribution of the noted error is not significant and can be considered as acceptable. An error of resulting density value, which comes out from hand sample submersion is expected to be not larger than ±1% for sample weight 0.5 kg, and not larger than ±0.5% for sample weight 1 kg.

Another source of error in measurements of density is brine/water draining from ice sample. In the paper it was studied how brine/water loss can influence the resulting density value. For the studied samples of 0.035 m thick the density variation was up to 0.5% in 1 min due to the brine/water loss.

The cumulative amount of water drained from the samples during 50-second time period corresponded to logarithmic law. Speed of water drainage was increased approximately two times after sample submersion. The amount of drained water noticeably increased with increased ice thickness, as it was expected.

The paper provides the results of model ice density measurements performed in the ice tank of Krylov State Research Centre (St. Petersburg). The increased model ice density observed in the experiments along with the increased water salinity, which corresponds to the known results with natural sea ice.

ACKNOWLEDGMENTS

Authors wish to thank Dr. Alexey Dobrodeev for his help with conduction of experiments. Authors are grateful to program “5-100-2020” of Peter the Great St. Petersburg Polytechnic University for support.

REFERENCES

Cox, G.F.N and Weeks, W.F., 1983. Equations for Determining the Gas and Brine Volumes in Sea Ice Samples. *Journal of Glaciology* Vol. 29 No. 102, pp. 306-316.

ITTC, 2014. *Test Methods for Model Ice Properties*. Revision 2. 7.5-0.2-0.4-0.2. 1-19.

Li, Zhijun and Riska, Kaj, 2002. Index for estimating physical and mechanical parameters of model ice. *Journal of Cold Regions Engineering* Vol. 16 (2), pp. 72–82.

Loset, Sveinung, Shkhinek, Karl N., Gudmenstad, Ove and Hoyland, Knut, 2010. *Vozdeystvie lda na morskie I beregovye sooruzheniya* [Effect of ice on marine and coastal structures. St.Petersburg ,In Russian], Lan': St. Petersburg.

Petrich, Chris, Langhorne, Pat J. and Sun, Zhifa F, 2006. Modelling the interrelationships between permeability, effective porosity and total porosity in sea ice. *Cold Regions Science and Technology* Vol. 44, pp. 131–144.

Popov N.I., Fedorov, K.N., Orlov V.M., 1979. *Morskaja voda* [Sea Water. In Russian] Nauka: Moscow.

Pustogvar, Anna and Kulyakhtin, Anton, 2016. Sea ice density measurements. Method and uncertainties. *Cold Regions Science and Technology* Vol. 131, pp. 46 – 52.

Timco G. W. and Weeks W. F., 2010. A review of the engineering properties of sea ice. *Cold Regions Science and Technology* Vol. 60, pp. 107 – 129.

Timco, Gary W. and Frederking, Robert M.W., 1996. A review of sea ice density. *Cold Regions Science and Technology* Vol. 24, pp. 1-6.

Timofeev, Oleg Ya., Sazonov, Kirill E. and Dobrodeev, Alexey A., 2015. New Ice Basin of the Krylov State Research Centre. *Proceedings of the 23rd POAC conference*, Trondheim, Norway, June 14-18, 8 p.

Von Bock und Polach, Rudiger, Ehlers, Sören and Kujala, Pentti., 2013. Model-scale ice - Part A: Experiments. *Cold Regions Science and Technology* Vol., pp. 74–81.

Zvyagin, Petr, 2016. On autocorrelation of ice loads, measured in ice tank experiments. *Proceedings of the 35th ASME OMAE conference*. OMAE2016-54436. Busan, Korea. June 19-24, : pp. 6.